Front. Optoelectron. 2021, 14(4): 482–490
https://doi.org/10.1007/s12200-021-1217-1

RESEARCH ARTICLE

Rapid thermal evaporation for cadmium selenide thin-film solar cells

Kanghua LI[1*], Xuetian LIN[1,2*], Boxiang SONG[1], Rokas KONDROTAS[3], Chong WANG[1], Yue LU[1,2], Xuke YANG[1], Chao CHEN (✉)[1], Jiang TANG[1,2]

1 Sargent Joint Research Center, Wuhan National Laboratory for Optoelectronics (WNLO), School of Optical and Electronic Information, Huazhong University of Science and Technology, Wuhan 430074, China
2 China-EU Institute for Clean and Renewable Energy (ICARE), Huazhong University of Science and Technology, Wuhan 430074, China
3 State Research Institute, Center for Physical Sciences and Technology, Vilnius 02300, Lithuania

Abstract Cadmium selenide (CdSe) belongs to the binary II-VI group semiconductor with a direct bandgap of ~1.7 eV. The suitable bandgap, high stability, and low manufacturing cost make CdSe an extraordinary candidate as the top cell material in silicon-based tandem solar cells. However, only a few studies have focused on CdSe thin-film solar cells in the past decades. With the advantages of a high deposition rate (~2 μm/min) and high uniformity, rapid thermal evaporation (RTE) was used to maximize the use efficiency of CdSe source material. A stable and pure hexagonal phase CdSe thin film with a large grain size was achieved. The CdSe film demonstrated a 1.72 eV bandgap, narrow photoluminescence peak, and fast photoresponse. With the optimal device structure and film thickness, we finally achieved a preliminary efficiency of 1.88% for CdSe thin-film solar cells, suggesting the applicability of CdSe thin-film solar cells.

Keywords cadmium selenide (CdSe), rapid thermal evaporation (RTE), solar cells, thin film

1 Introduction

Silicon-based solar cells have dominated the photovoltaic market and are approaching their theoretical limiting efficiency (29.4%) for single-junction [1]. To break through the Shockley–Queisser limit for single-junction devices, a tandem structure is expected to realize the power conversion efficiency (PCE) of more than 40% for multijunction solar cells [2]. Theoretically, a top cell with a bandgap of ~1.7 eV is preferred to match silicon (Si, 1.12 eV) bottom-cell and can achieve a high PCE of up to 45% in a tandem solar cell [3]. In a monolithic tandem structure, two PN junctions made of one wide-bandgap material and one narrow-bandgap material are series-connected to minimize the energy loss caused by thermal relaxation and produce higher PCE. Even many materials have been explored as the top cells in Si-based tandem devices, there are still various challenges in extensive commercial applications [4]. III-V semiconductors are not suitable for large-scale terrestrial photovoltaic commercial use owing to the high fabrication cost [5]. The bottleneck for perovskite top cells is that the stability has not met the requirement for practical application [6]. With a bandgap of 1.47 eV, the intrinsic cadmium telluride (CdTe) is incompatible with Si-based tandem solar cells [7]. Other than the advantages of good stability and low cost, cadmium selenide (CdSe) has an appropriate bandgap of ~1.7 eV and provides great potential in Si-based tandems.

With simple binary composition, CdSe has an appropriate bandgap of 1.72 eV [8] and high absorption coefficient in the visible light range [9]. Similar to other II-VI group compounds, it demonstrates excellent optoelectronic properties, which are widely used in light-emitting diodes (LED) [10] and photodetector [11]. However, CdSe has rarely been studied as a potential photovoltaic material in the past. One of the technical challenges is how to obtain highly crystallized CdSe films with low defect density. Furthermore, as an n-type semiconductor [12], finding a suitable p-type candidate is important to build a high-quality PN junction with CdSe thin film. Solving the above problems well, CdSe can be potentially used as a top subcell in tandem Si-based devices.

In a rapid thermal evaporation (RTE) system, the powdered source material is evaporated and deposited on

Received March 22, 2021; accepted April 1, 2021

E-mail: cchen@mail.hust.edu.cn

*These authors contributed equally.

the substrate located within 10 mm from the source. This design in the RTE system allows high deposition rates (~2 μm/min), effective use of source materials, high uniformity in thickness and composition of thin films. Therefore, RTE has been successfully used in synthesizing photovoltaic-grade thin films, such as Sb_2Se_3 [13], Sb_2S_3 [14], Bi_2S_3 [15], and GeSe [16]. Similar to those chalcogenides, CdSe has high saturated vapor pressure, which facilitates the deposition via the RTE method [17].

Here, we demonstrated the application of the RTE method to deposit CdSe thin films with large grain size and pure phase. The CdSe thin film exhibited a bandgap of 1.72 eV and good light response. Through the design of the device structure and optimization of CdSe film thickness, 1.88% conversion efficiency was achieved in CdSe thin-film solar cells. The RTE deposited CdSe thin-film solar cells here show great potential in Si-based tandem solar cell application.

2 Experimental section

2.1 CdSe solar cell fabrication

The fluorine doped tin oxide (SnO_2:F, FTO) transparent conductive glasses were purchased (OPV Tech). The thickness, transmittance, and sheet resistance of the FTO layer are 500 nm, > 85% (400–800 nm), and 8 Ω/sq, respectively. FTO was rinsed in the ultrasonic cleaning machine by the following solvent: detergent, acetone, isopropanol, ethyl alcohol, and deionized water in sequence. Titanium dioxide (TiO_2) thin film was prepared using spray pyrolysis. The precursor solution used for spraying consisted of titanium diisopropoxide bis (acetylacetonate) (75 wt.% in isopropanol, Aladdin) and anhydrous ethanol (99.99% purity, Aladdin) in a ratio of 1:9. While spraying, the temperature and constant flow rate were 450°C and 12 mL/min, respectively. First, TiO_2 was annealed on the hotplate at 450°C for 30 min in ambient air. Zinc oxide (ZnO) was prepared based on a previously reported solgel method [18]. 0.4-mol/L zinc acetate dihydrate and monoethanolamine (1:1 molar ratio) were dissolved in 2-methoxy ethanol solution and stirred at 60°C for 12 h. Then, the ZnO sol was dipped onto the FTO and spun at 3000 r/min for 30 s, following the annealing treatment at 500°C for 20 min. Cadmium sulfide (CdS) film was prepared via chemical bath deposition for 16 min on the substrate. Then, the CdS film was treated with 20 mg/mL cadmium chloride ($CdCl_2$) absolute methanol solution via spin coating and annealed on the hotplate at 400°C for 6 min in ambient air. Rapid thermal evaporation (RTE, OTF-1200X-RTP, Hefei) was used for depositing CdSe films by evaporating CdSe powder (99.995% purity, Alpha). During the specific operation process: 0.5-g CdSe powder was evenly placed on the 5 cm × 5 cm × 0.1 cm quartz glass in the center of the RTE. The substrate was put 10 mm above the source. To maintain the low temperature of the substrate, a graphite block with a large heat capacity was placed on top of it. After pumping the pressure below 1 Pa, we first preheated the RTE system at 400°C for 900 s, then rapidly increased the temperature to 800°C at a ratio of 20°C/s and kept it for different periods (50, 100, and 150 s) to deposit the CdSe films.

PEDOT-4083 (Xi'an Polymer Light Technology Co., China) with less than 0.5% TOYNOL Super wet-340 Surfactant (Tianjin SurfyChem T&D Co., Ltd., China) was deposited on the CdSe film by spin-coated method at 3000 r/min for 30 s. Subsequently, to remove the residual solvent, it was annealed at 150°C for 10 min on the hotplate. Copper iodide (CuI, 98% purity, Aladdin) was dissolved in diethyl sulfide (99% purity, Aladdin) with a concentration of 10 mg/mL. Then, the CuI precursor was spincoated at 3000 r/min for 30 s to deposit CuI film. Au electrodes (0.09 cm^2) were deposited using a resistance evaporation thin-film deposition system (Beijing Technol Science Co., Ltd., China) under a vacuum pressure of 5 × 10^{-3} Pa.

2.2 Materials characterizations

Scanning electron microscopy (SEM, FEI Nova Nano-SEM450, without Pt coating) images were used to study the morphologies of CdSe films. The phase and orientation of CdSe films were determined using the X-ray diffraction (XRD) with Cu Kα radiation (Philips, X pert pro-MRD). UV–Vis spectrophotometer (PerkinElmer Instruments, Lambda 950 using integrating sphere) was conducted to determine the optical transmittance of CdSe thin-films. Photoluminescence (PL) spectra were measured using a confocal Raman microscope (LabRAM HR800, HORIBA, Ltd., France) with a 532-nm excitation wavelength at 100 multiples attenuation. The valence band and Fermi level of CdSe film were measured using ultraviolet photoelectron spectroscopy (UPS) (Specs UVLS, HeI excitation, 21.21 eV, referenced to the Fermi edge of argon etched gold).

2.3 Device characterizations

Current–voltage (*I–V*) curves were measured under the bias voltage varying from – 1 to 1 V at 25°C under dark or light (530 nm, 500 Ma, 5 mW/cm^2) conditions. Under 1-V bias voltage, the photoelectric response of CdSe/gold (Au) was measured with a 530-nm light illumination and a 10-s signal circumference. The current-density–voltage (*J–V*) characterization was obtained using a source meter (Keithley 2400) under the dark conditions and simulated AM 1.5G (100 mW/cm^2) illumination (Oriel, Model 9119, Newport). For external quantum efficiency (EQE) measurement, a light source generated using a 300 W xenon

lamp of Newport (Oriel, 69911) was used and it was split into a specific wavelength using Newport oriel cornerstone TM 130 1/8 Monochromator (Oriel, model 74004).

3 Results and discussion

RTE is a similar thin-film deposition technology to the well-known closed-space sublimation (CSS) [19,20]. The main difference lies in the equipment design. RTE has a single heating source, whereas in CSS substrate and source are heated separately. It has the advantages of fast film formation, good film uniformity, high material utilization, and pure phase of the prepared materials. Theoretically, high-quality CdSe films can be prepared using RTE using the sublimation property of CdSe. The schematic diagram of RTE is shown in Fig. 1(a). The CdSe powder was uniformly scattered on the quartz glass, and the FTO substrate was placed above the CdSe powder (10-mm distance) with a graphite block on the top. The graphite block is used to minimize the variation of the substrate temperature during the evaporation. From the plot of saturation vapor pressure with temperature (Fig. 1(b)), it requires exceeding 1023 K and reach >1 Pa vapor pressure to evaporate CdSe. Based on the above analysis, the target evaporation temperature was set as 740 K to obtain enough CdSe vapor. The CdSe powder decomposes into element Se_2 and Cd at high temperatures, as seen in Eq. (1).

$$\mathrm{CdSe} \rightleftharpoons \mathrm{Cd}\ (\mathrm{g}) + (1/2)\ \mathrm{Se}_2(\mathrm{g}) \qquad (1)$$

At low temperatures, Cd and Se_2 will react and form CdSe vapor [17]. This deposition mechanism makes it difficult for CdSe to introduce impurities in the deposition process [17]. Moreover, it is beneficial to the growth of CdSe grains, thus improving the crystallinity of CdSe films. The similar saturation vapor pressure of Cd and Se can enable an approximately stoichiometric ratio during the evaporation process. Eventually, the Cd and Se_2 vapor combine to form CdSe and condense on the low-temperature FTO substrate.

The XRD (Fig. 1(c)) was performed to characterize the phase purity of the as-prepared CdSe films. Furthermore, the CdSe and remaining powders after RTE evaporation were tested as reference samples. The prominent XRD peaks (100), (002), (101), (110), (103), and (112) of the powder samples correspond to the hexagonal crystal structure (JCPDS: 00-008-0459) [21]. These demonstrate that CdSe evaporated congruently and no phase separation or selective evaporation occurred. As for the deposition of CdSe thin films, elemental Cd or Se peaks were not observed in the XRD pattern of CdSe films (Fig. 1(c)), even the vapor pressure of Se and Cd is much lower than CdSe. The X-ray photoelectron spectroscopy (XPS) was performed to characterize the chemical valency of the Cd and Se in the CdSe film (Fig. S1). The only Cd^{2+} and Se^{2-} in the surface and bulk of CdSe indicate the no remain of elemental Cd or elemental Se. CdSe thin films show a single characteristic peak of (103), which is consistent with the hexagonal crystal structure. The single orientation, stable hexagonal crystal, and pure phase in the prepared CdSe thin films indicate high crystal quality.

The basic optoelectronic properties were characterized to further study the quality of CdSe thin films. The steep absorption edge in the absorption spectra suggests that CdSe is a direct bandgap semiconductor (Fig. 2(a)). From the Tauc plot [22], a direct bandgap of 1.72 eV was obtained by extrapolating the linear region to the x-axis (Fig. S2). The obtained value agrees well with the values found for single crystals (1.72 eV) [23]. Photoluminescence (PL) of CdSe was measured at 25°C. It shows a strong and narrow PL peak located around 713 nm (1.74 eV). The full-width half-maximum (FWHM) of PL peak is 23 nm (0.0185 eV). We also analyzed the PL spectrum more carefully, focusing on the wavelength >800 nm. The PL of CdSe overlaps with the background (Fig. S3), indicating fewer defects exist in the as-prepared CdSe films. Further, it indicates the absence of near band-edge defects and high quality of the films.

To determine the band position of the conduction band minimum and valence band in CdSe thin film, UPS

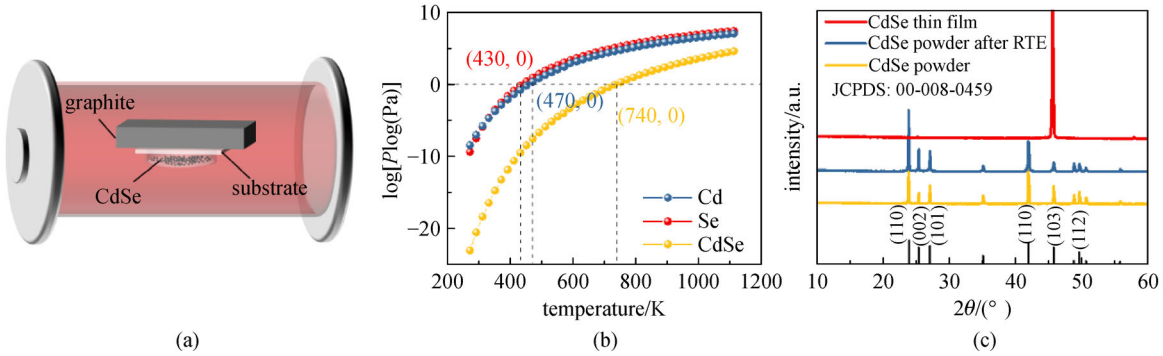

Fig. 1 (a) Schematic diagram of RTE. (b) Curves of the saturation vapor pressure of Cd, Se, and CdSe with temperature. (c) XRD spectra of CdSe powder and thin film

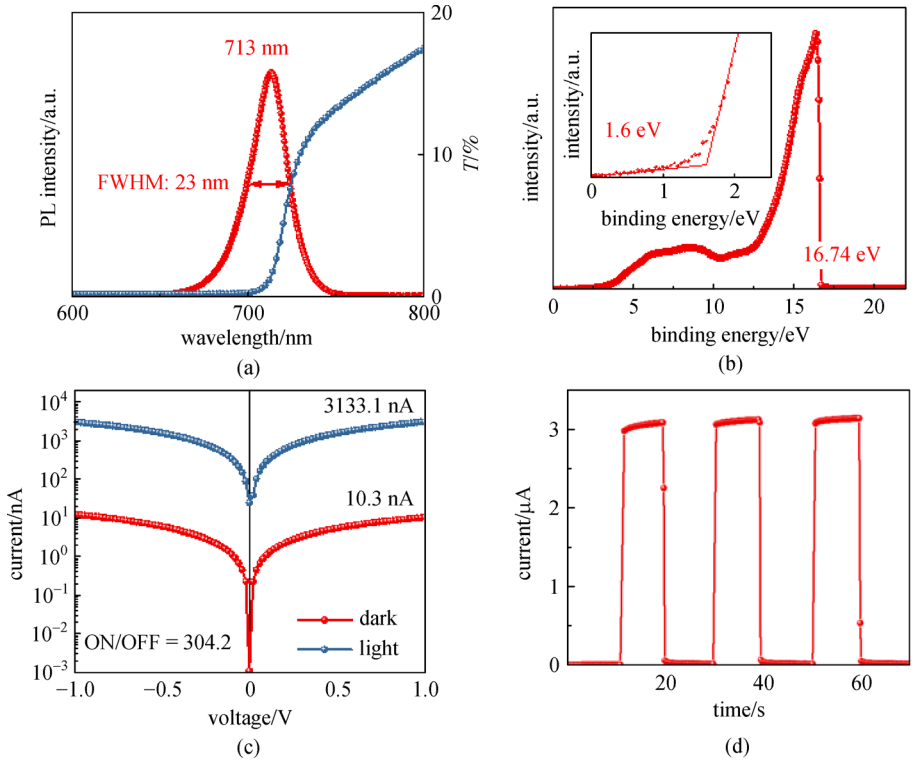

Fig. 2 Optoelectronic properties of CdSe films. (a) Transmittance and PL spectra of CdSe thin film. (b) UPS spectra of CdSe thin film. The inset is the zoom-in image in the range of 0–2.5 eV. (c) *I–V* curves and (d) *I–t* curve of CdSe photo-conductance type detector under dark and 530 nm LED illumination

characterization was further conducted (Fig. 2(b)). We found that the ionization potential and Fermi level of CdSe thin films were located at 6.07 and 4.47 eV, respectively. Combining the bandgap of 1.72 eV, the electron affinity is found to be at 4.35 eV. The Fermi level is located near the conduction band, implying the n-type nature of CdSe [24]. The n-type feature originates from the Se vacancy defects during the deposition process [25,26].

To study the photoresponse properties and test the suitability for optoelectronic applications, CdSe/Au was deposited on insulating glass substrates under the same conditions as in CdS/FTO substrate. The SEM and XRD (Fig. S4) show the similar quality of CdSe thin film on the CdS/FTO and glass substrates. A constant bias of 1 V was applied between electrodes, and a 530-nm wavelength LED was used as an excitation source. Under dark conditions, the current was approximately 10 nA, which indicated low conductivity (5×10^4 Ω) of the CdSe thin films [27]. The specific calculation process is in the Electronic Supplementary Material. High resistivity is common for II-VI group materials without doping, such as CdTe [28] and CdS [29]. Under illumination, the conductivity increased significantly with an ON/OFF ratio of 304 (~5 mW/cm^2) (Fig. 2(c)), which indicated that the CdSe film had an excellent optoelectronic performance. Furthermore, the current rise and fall durations were within 0.2 s (Figs. 2(d) and S5). The fast light response suggests a low density of deep defects and fewer intrinsic bulk defects in CdSe film [30]. Overall, the deposited CdSe thin film is of high quality and highly photosensitive, therefore it is suitable for working as an absorbing layer.

To construct CdSe thin-film solar cells, suitable hole transport layers (HTLs) and electron transport layers (ETLs) need to be identified (Fig. 3(a)). Benefiting from the HTL and ETL, the photogenerated carriers can be efficiently separated and subsequently collected by the electrodes. The HTL should have a higher conduction band to block the migration of photogenerated electrons to the HTL and reduce recombination with holes at the CdSe/HTL interface. Similarly, the ETL needs to have a deeper valence band to block photogenerated holes (Fig. 3(b)). The CdSe is an n-type layer, then the p-type HTL is significant to build a PN junction. As shown in Fig. 3(c), we have made some attempts in HTL and CdS is used as an ETL. CuI is a typical wide-bandgap p-type material with high carrier concentration, and high mobility serving as an HTL in solar cells [31]. The CdSe solar cell with CuI demonstrates a high short-circuit current (J_{SC}) exceeds 4 mA/cm^2. Nevertheless, the open-circuit voltage (V_{OC}) of the device is only 0.1 V, which might be caused by the interface defects. Polymers are considered to form good interfaces. The devices with PEDOT as HTL achieves a high V_{OC} of 0.4 V. However, the high resistance of the

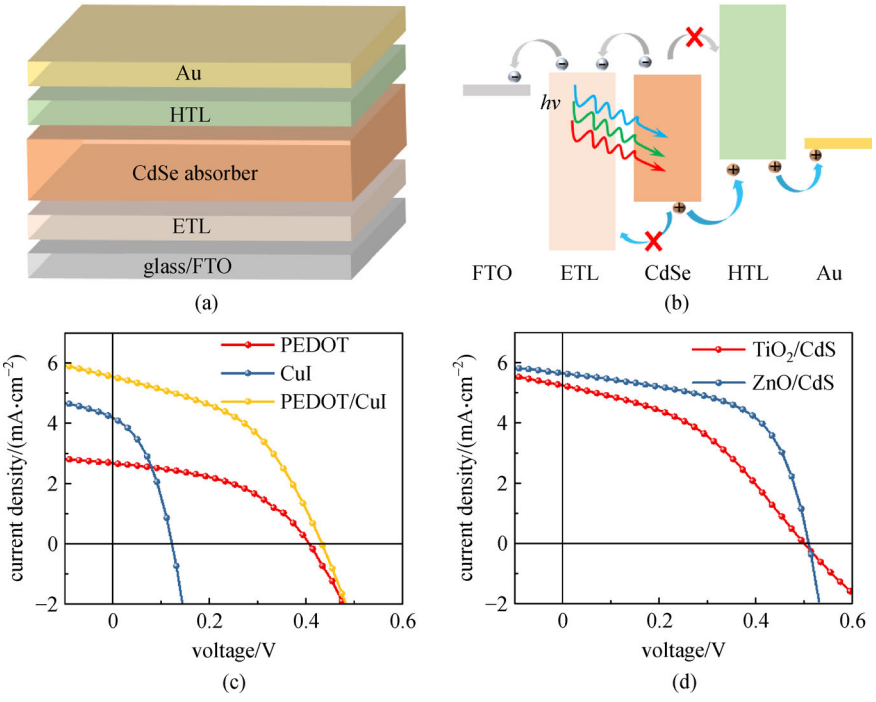

Fig. 3 (a) Device structure schematic of CdSe thin-film solar cell. (b) Schematic diagram of energy band structure and charge transfer in CdSe solar cell. (c) *J–V* curves of CdSe solar cells with PEDOT, CuI, and PEDOT/CuI as HTL. (d) *J–V* curves of CdSe solar cells with TiO_2/CdS and ZnO/CdS as ETL

PEDOT might not be favorable for carriers' transport, resulting in a low J_{SC} of 2.8 mA/cm^2. Then, we designed a dual-hole collection layer (PEDOT/CuI). Consequently, the CdSe solar cell device exhibited a significant improvement in photogenerated carrier collection. Finally, we obtained an efficiency of 0.74% with high J_{SC} (5.5 mA/cm^2) and high V_{OC} (0.45 V) (Fig. 3(c)).

Furthermore, the interfacial energy level mismatch in the FTO/CdS could limit the performance of CdSe solar cells, particularly the fill factor (FF). Moreover, the CdS buffer layer might react during CdSe film deposition. It might lead to the direct contact of the CdSe film with the FTO electrode and result in leakage [32]. A thin TiO_2 layer was introduced at the FTO/CdS interface as a barrier layer. The *J–V* curve of the device is shown in Fig. 3(d), and the V_{OC} of the device is raised to 0.51 V. However, the high resistance of TiO_2 might impede carrier transport to some extent and increase the resistance. Moreover, the conduction band energy level mismatch of TiO_2 and CdSe leads to a kink phenomenon in the *J–V* curve. To address those issues, the TiO_2 layer was replaced by the ZnO layer with lower resistance, leading to the enhancement of charge transfer and the reduction of interfacial recombination [33]. As a result, a high FF of 58%, a high V_{OC} of 0.51 V, and a PCE of 1.45% were obtained in the device with ZnO/CdS as ETLs.

In addition to HTL and ETL, the thickness of CdSe directly affects its light absorption and the transport of photogenerated carriers. By adjusting the deposition time, we could control the thickness of the CdSe absorber layer. As the increasing deposition time from 50 to 150 s, the grain size of CdSe films increases from 560 to 2390 nm (Figs. 4(a)–4(c)), and the thickness of the increases from 500 to 2900 nm (Figs. 4(d)–4(f)). There is a good linear relationship between film thickness and deposition time (Fig. S6), which is more conducive to accurate control of the thickness of CdSe film. Furthermore, the SEM cross-sectional view shows that the CdSe grains also grow continuously upward from the substrate.

For brevity, we define the devices with CdSe thicknesses of 500, 1800, and 2900 nm as D500, D1800, and D2900, respectively. As shown in Fig. 5(a), the efficiency of CdSe thin-film solar cell decreased with the increase of the film thickness. A champion efficiency of 1.88% was obtained in the D500. The PCEs of D1800 and D2900 are 0.73% and 0.02%, respectively (Table 1). On one hand, the large absorption coefficient of CdSe was confirmed because film with hundreds of nanometers thickness demonstrated a good absorption. On the other hand, it illustrated that minority diffusion is difficult with the increase of absorption layer thickness, leading to a loss of J_{SC}. The significant reduction in J_{SC} decreases PCE. We measured the EQE to study the reason for the J_{SC} reduction (Fig. 5(b)). All devices exhibit better long-wave EQE response, implying better carrier transport at the CdSe/HTL interface. The short-wavelength EQE response decreases significantly or even to 0 with increasing film thickness, because of the problematic carrier transport

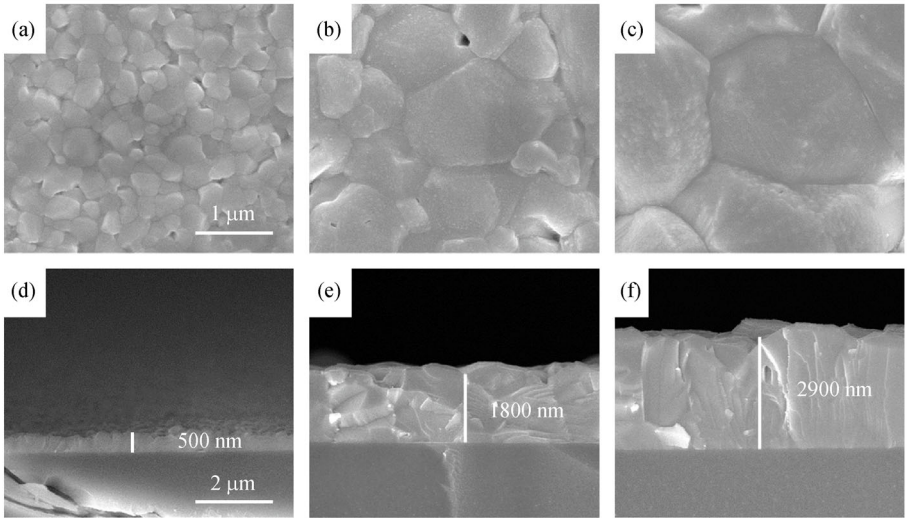

Fig. 4 (a)–(c) Surface SEM images and (d)–(f) cross-sectional SEM images of CdSe thin film with different thicknesses

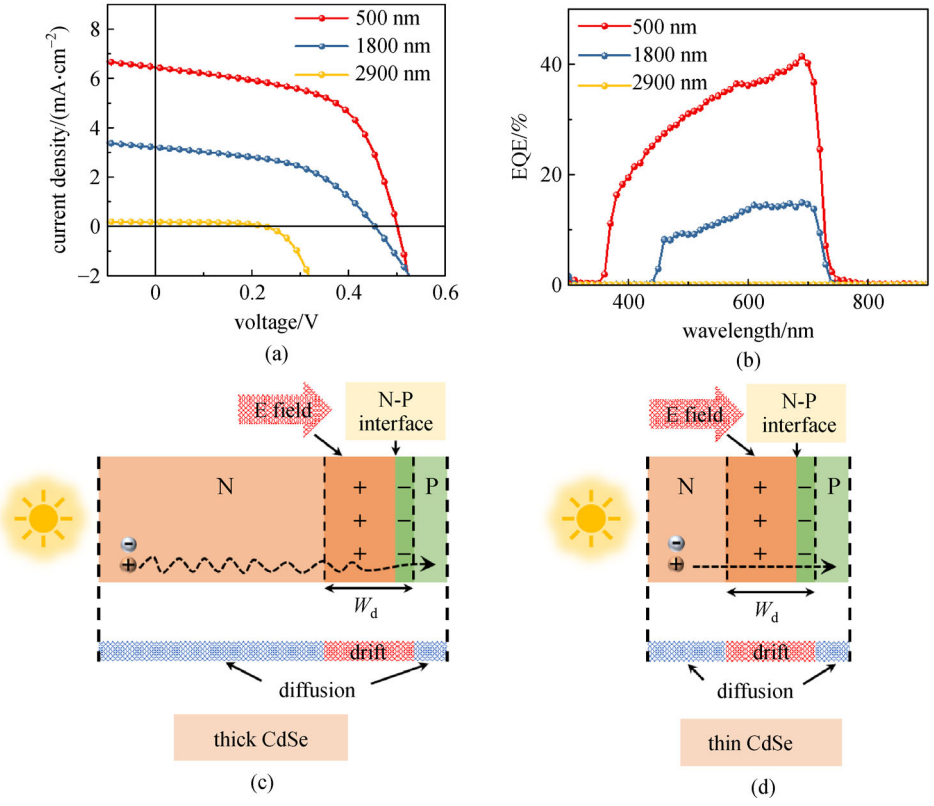

Fig. 5 (a) *J*–*V* curves and (b) EQE spectra of CdSe thin-film solar cells with different CdSe thickness. The schematic diagram of holes collection as minority light generated carrier in (c) the thick device and (d) the thin device

close to the ETL/CdSe interface.

To clarify possible reasons, we infer that the main PN junction is formed at the CdSe/HTL interface. Under the influence of the electric field, the carriers are separated rapidly and collected by the electrode. However, the photogenerated electrons and holes near the CdSe/ETL interface can only be collected by diffusion. Recombining is easy for electrons and holes photogenerated in the diffusion process. With the increase of absorption layer thickness, the photogenerated electrons and holes have a higher risk of being recombined. For a device with a thicker CdSe film, the photogenerated holes at the ETL/CdSe interface need to travel a longer diffusion distance and are easily recombined with electrons (Fig. 5(c)). For a

Table 1 Device performance of CdSe solar cell with different thicknesses

thickness/nm	V_{OC}/V	J_{SC}/(mA·cm^{-2})	FF/%	PCE/%
500	0.501	6.45	58.1	1.88
1800	0.454	3.23	50.0	0.73
2900	0.222	0.17	53.1	0.02

device with a thinner CdSe film, the holes can quickly enter the space charge area and be effectively collected (Fig. 5(d)). Hence, in devices with thicker CdSe, the short-wavelength EQE is sharply reduced and the J_{SC} is smaller.

4 Conclusion

In summary, the CdSe thin film was obtained by the RTE process with high quality, which is confirmed via the large grain size, single strong (103) peak, and high photo-response. After designing a structure of FTO/ETLs/CdSe/HTLs/Au, we obtained a PCE of 1.88% in CdSe solar cell through the thickness optimization of CdSe. This is a preliminary exploration and demonstration of the feasibility of CdSe thin-film solar cells. Further effort is required to focus on solving the problem of carrier transport at the ETL/CdSe interface, to improve J_{SC}, which will enhance the efficiency of CdSe solar cells to a new level. This work also paves the way for the in-depth study of CdSe thin-film solar cells and their application toward tandem solar cells.

Acknowledgements This work was supported by the National Natural Science Foundation of China (Grant Nos. 61725401, 61904058, and 62050039), the National Key R&D Program of China (No. 2016YFA0204000), the Innovation Fund of WNLO, National Postdoctoral Program for Innovative Talent (No. BX20190127), the Graduates' Innovation Fund of Huazhong University of Science and Technology (No. 2020yjsCXCY003), and China Postdoctoral Science Foundation Project (Nos. 2019M662623 and 2020M680101). The authors thank the Analytical and Testing Center of HUST and the facility support of the Center for Nanoscale Characterization and Devices (CNCD), WNLO-HUST.

Electronic Supplementary Material Supplementary material is available in the online version of this article at https://doi.org/10.1007/s12200-021-1217-1 and is accessible for authorized users.

References

1. Hermle M, Feldmann F, Bivour M, Goldschmidt J C, Glunz S W. Passivating contacts and tandem concepts: Approaches for the highest silicon-based solar cell efficiencies. Applied Physics Reviews, 2020, 7(2): 021305–021312
2. Meillaud F, Shah A, Droz C, Vallat-Sauvain E, Miazza C. Efficiency limits for single-junction and tandem solar cells. Solar Energy Materials and Solar Cells, 2006, 90(18–19): 2952–2959
3. Rickus D B E. The CdSe thin-film solar cell. Conference Record of the IEEE Photovoltaic Specialists Conference, 1980, 1: 629–632
4. Lu S, Chen C, Tang J. Possible top cells for next-generation Si-based tandem solar cells. Frontiers of Optoelectronics, 2020, 13(3): 246–255
5. Yamaguchi M, Lee K H, Araki K, Kojima N. A review of recent progress in heterogeneous silicon tandem solar cells. Journal of Physics D, Applied Physics, 2018, 51(13): 133002–133015
6. Todorov T, Gunawan O, Guha S. A road towards 25% efficiency and beyond: perovskite tandem solar cells. Molecular Systems Design & Engineering, 2016, 1(4): 370–376
7. Todorov T K, Bishop D M, Lee Y S. Materials perspectives for next-generation low-cost tandem solar cells. Solar Energy Materials and Solar Cells, 2018, 180: 350–357
8. Bakiyaraj G, Dhanasekaran R. Effect of annealing on the properties of chemical bath deposited nanorods of CdSe thin films. Crystal Research and Technology, 2012, 47(9): 960–966
9. Bagheri B, Kottokkaran R, Poly L P, Sharikadze S, Dalal V. Efficient heterojunction thin film CdSe solar cells deposited using thermal evaporation. In: Proceedings of IEEE 46th Photovoltaic Specialists Conference (PVSC). Chicago: IEEE, 2019, 1822–1825
10. Che S B, Nomura I, Kikuchi A, Shimomura K, Kishino K J P S S. Visible light emitting diode with ZnCdSe/BeZnTe superlattices as an active layer and MgSe/BeZnTe superlattices as a p-cladding layer. Physica Status Solidi (B): Basic Solid State Physics, 2002, 229(2): 1001–1004
11. Jia S, Yun X, An Y, Li P, Xiao J. Fabrication and characterization of photo-detector based on $CdSe_{0.5}S_{0.5}$ quantum dots. Asia Communications & Photonics Conference, 2013, 2013: 978–981
12. Mahawela P, Jeedigunta S, Vakkalanka S, Ferekides C S, Morel D L J T S F. Transparent high-performance CdSe thin-film solar cells. Thin Solid Films, 2005, 480–481(3): 466–470
13. Wang C, Du X, Wang S, Deng H, Chen C, Niu G, Pang J, Li K, Lu S, Lin X, Song H, Tang J. Sb_2Se_3 film with grain size over 10 μm toward X-ray detection. Frontiers of Optoelectronics, 2020, doi:10.1007/s12200-020-1064-5
14. Shin Y M, Lee C S, Shin D H, Kwon H S, Park B G, Ahn B T. Surface modification of CIGS film by annealing and its effect on the band structure and photovoltaic properties of CIGS solar cells. Current Applied Physics, 2015, 15(1): 18–24
15. Song H, Zhan X, Li D, Zhou Y, Yang B, Zeng K, Zhong J, Miao X, Tang J. Rapid thermal evaporation of Bi_2S_3 layer for thin film photovoltaics. Solar Energy Materials and Solar Cells, 2016, 146: 1–7
16. Xue D J, Liu S C, Dai C M, Chen S, He C, Zhao L, Hu J S, Wan L J. GeSe thin-film solar cells fabricated by self-regulated rapid thermal sublimation. Journal of the American Chemical Society, 2017, 139 (2): 958–965
17. Somorjai G A. Vapor pressure and solid-vapor equilibrium of CdSe (cadmium selenide). Journal of Physical Chemistry, 1961, 65(6): 1059–1061
18. Li K, Kondrotas R, Chen C, Lu S, Wen X, Li D, Luo J, Zhao Y, Tang J. Improved efficiency by insertion of $Zn_{1-x}Mg_xO$ through sol-gel method in ZnO/Sb_2Se_3 solar cell. Solar Energy, 2018, 167: 10–17
19. Major J D, Proskuryakov Y Y, Durose K. Impact of CdTe surface composition on doping and device performance in close space sublimation deposited CdTe solar cells. Progress in Photovoltaics,

2013, 21(4): 436–443
20. Gnatenko Y P, Bukivskij P M, Faryna I O, Opanasyuk A S, Ivashchenko M M. Photoluminescence of high optical quality CdSe thin films deposited by close-spaced vacuum sublimation. Journal of Luminescence, 2014, 146: 174–177
21. Tian L, Yang H, Ding J, Li Q, Mu Y, Zhang Y. Synthesis of the wheat-like CdSe/CdTe thin film heterojunction and their photovoltaic applications. Current Applied Physics, 2014, 14(6): 881–885
22. Chen C, Zhao Y, Lu S, Li K, Li Y, Yang B, Chen W, Wang L, Li D, Deng H, Yi F, Tang J. Accelerated optimization of TiO_2/Sb_2Se_3 thin film solar cells by high-throughput combinatorial approach. Advanced Energy Materials, 2017, 7(20): 1700866
23. Parsons R B, Wardzynski W, Yoffe A D. The optical properties of single crystals of cadmium selenide. Proceedings of the Royal Society of London. Series A, Mathematical and Physical Sciences, 1961, 262(1308): 120–131
24. Rosly H N, Rahman K S, Harif M N, Doroody C, Isah M, Misran H, Amin N. Annealing temperature assisted microstructural and optoelectrical properties of CdSe thin film grown by RF magnetron sputtering. Superlattices and Microstructures, 2020, 148: 106716
25. Ni Z H, Kong B, Zeng T X, Yang H, He Z Y. The effects of the intrinsic defects on the electronic, magnetic and optical properties for bulk and monolayer CdSe: first-principles GGA + U investigations. Materials Research Express, 2019, 6(10): 105903
26. Murali K R, Srinivasan K, Trivedi D C. Vacuum evaporated CdSe thin films and their characteristics. Materials Letters, 2005, 59(1): 15–18
27. Murali K R, Srinivasan K, Trivedi D C. Structural and photoelectrochemical properties of CdSe thin films deposited by the vacuum evaporation technique. Materials Science and Engineering B, 2004, 111(1): 1–4
28. Kosyak V, Opanasyuk A, Bukivskij P M, Gnatenko Y P. Study of the structural and photoluminescence properties of CdTe polycrystalline films deposited by close-spaced vacuum sublimation. Journal of Crystal Growth, 2010, 312(10): 1726–1730
29. Hariskos D, Powalla M, Chevaldonnet N, Lincot D, Schindler A. Chemical bath deposition of CdS buffer layer: prospects of increasing materials yield and reducing waste. Thin Solid Films, 387(1–2): 179–181
30. Leng M Y, Luo M, Chen C, Qin S K, Chen J, Zhong J, Tang J. Selenization of Sb_2Se_3 absorber layer: an efficient step to improve device performance of CdS/Sb_2Se_3 solar cells. Applied Physics Letters, 2014, 105(8): 083905
31. Hu W D, Dall'Agnese C, Wang X F, Chen G, Li M Z, Song J X, Wei Y J, Miyasaka T. Copper iodide-PEDOT:PSS double hole transport layers for improved efficiency and stability in perovskite solar cells. Journal of Photochemistry and Photobiology A Chemistry, 2018, 357: 36–40
32. Voswinckel S, Mikolajick T, Wesselak V. Influence of the active leakage current pathway on the potential induced degradation of CIGS thin-film solar modules. Solar Energy, 2020, 197: 455–461
33. Wang L, Li D B, Li K, Chen C, Deng H X, Gao L, Zhao Y, Jiang F, Li L, Huang F, He Y, Song H, Niu G, Tang J. Stable 6%-efficient Sb_2Se_3 solar cells with a ZnO buffer layer. Nature Energy, 2017, 2 (4): 17046–17053

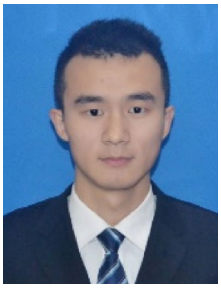

Kanghua Li received his Bachelor's degree from Huazhong University of Science and Technology, China in 2015. Then he studied in Wuhan National Laboratory for Optoelectronics, Huazhong University of Science and Technology as a doctoral candidate and received his Ph.D. degree in 2020. Currently, he is a post-doctor in Wuhan National Laboratory for Optoelectronics at Huazhong University of Science and Technology, China. His research interests are thin-film solar cells and photodetectors.

Xuetian Lin is a candidate for a Master's degree at Huazhong University of Science and Technology (HUST, China) and Paris Sciences & Lettres University (France). She majors in New Energy Science and Technology in China-EU Institute for Clean and Renewable Energy in HUST. She also majors in Clean and Renewable Energy in the MINES ParisTech of PSL University (France). She mainly works on photovoltaic materials.

Boxiang Song received his B.S. degree (2012) from Nanjing University (China), M.S. degree (2014) from University of Pennsylvania (USA), and Ph.D. degree (2019) from University of Southern California (USA) under the supervision of Prof. Wei Wu. After one-year of postdoctoral research at University of Southern California, he joined Wuhan National Laboratory for Optoelectronics, Huazhong University of Science and Technology, as a full-time professor. His research interests include nanofabrication, plasmonics, and metamaterials. Specifically, he pioneered the gap plasmonic nanostructure with sub-nanometer accuracy in large periodic arrays for precise chemical detection. He has published more than 20 papers, including *Science Robotics*, *ACS Nano*, and *Small*. He is a member of the IEEE Nanotechnology Council, and the invited reviewer for *Nanophotonics*, *Nanoscale*, and *Applied Physics A*.

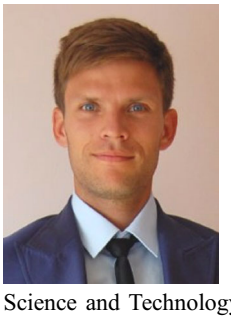

Rokas Kondrotas earned his Ph.D. degree in Center for Physical Sciences and Technology jointly with Vilnius University, Lithuania in 2015. Then he worked as a post-doctor in Catalonia Institute for Energy Research, Spain for one year. Afterward, he joined Prof. Jiang Tang's group in Wuhan National Laboratory for Optoelectronics at Huazhong University of Science and Technology, China. After his second post-doc, Rokas

returned to Center for Physical Science and Technology where now he is employed as a senior researcher. His research is focused on the fabrication and study of thin-film solar cells, including $Cu_2ZnSnSe_4$, $Cu(In,Ga)Se_2$, and Sb_2Se_3.

Chong Wang received his Bachelor's degree (2015) and Ph.D. degree (2020) in Optical Engineering from Wuhan National Laboratory for Optoelectronics, Huazhong University of Science and Technology, China. Now his research interests are novel semiconductor optoelectronic materials and devices.

Yue Lu received his Bachelor's degree from China University of Geosciences (Wuhan), China in 2019. He is currently pursuing his M.S. degree from both Huazhong University of Science and Technology (China) and the MINES ParisTech of PSL University (France). He also a master student, major in Clean and Renewable Energy in the MINES ParisTech of PSL University (France). His current research interests focus on thin-film solar cells and photodetectors.

Xuke Yang started his studies in School of Optics and Electronic Information, Huazhong University of Science and Technology, China in 2017, and he will receive a bachelor's degree from Huazhong University of Science and Technology, China in 2021. Since August 2020, he has been conducting research and studies at Wuhan National Laboratory for Optoelectronics, Huazhong University of Science and Technology, China. His research interests are thin solar cells and photodetectors.

Chao Chen received his B.S. degree in School of Physics at Huazhong University of Science and Technology (HUST), China in 2014. From 2014/09 to 2019/02, he studied in Wuhan National Laboratory for Optoelectronics at HUST as a doctoral candidate and received his Ph.D. degree in 2019. From 2019/02 to 2021/02, he worked in Wuhan National Laboratory for Optoelectronics as a post-doctor. Recently, he joined School of Optical and Electronic Information, HUST as an associate professor. His research interests are thin-film solar cells and photodetectors.

Jiang Tang is a professor at Wuhan National Laboratory for Optoelectronics, Huazhong University of Science and Technology, China. He obtained his Ph.D. degree from University of Toronto, Canada in 2010. His research interest is optoelectronic devices including X-ray and infrared detectors, thin-film solar cells, and light-emitting diodes. He has published >150 papers, filed >30 patents.